Scientific Research Publishing

Advances in Materials Physics and Chemistry, 2018, 8, 193-215
http://www.scirp.org/journal/ampc
ISSN Online: 2162-5328
ISSN Print: 2162-531X

$LaMnO_3$ ($La_{0.8}Sr_{0.2}MnO_3$) Perovskites for Lean Methane Combustion: Effect of Synthesis Method

Natalia Miniajluk[1,2*], Janusz Trawczyński[1], Mirosław Zawadzki[2], Włodzimierz Tylus[3]

[1]Division of Chemistry and Technology of Fuels, Wroclaw University of Technology, Wrocław, Poland
[2]Institute of Low Temperature and Structural Research Polish Academy of Sciences, Wrocław, Poland
[3]Institute of Technology of Inorganic and Mineral Fertilizers, Wroclaw University of Technology, Wrocław, Poland
Email: *natalia.miniajluk@pwr.edu.pl; janusz.trawczynski@pwr.edu.pl, M.Zawadzki@int.pan.wroc.pl, w.tylus@pwr.edu.pl

How to cite this paper: Miniajluk, N., Trawczyński, J., Zawadzki, M. and Tylus, W. (2018) $LaMnO_3$ ($La_{0.8}Sr_{0.2}MnO_3$) Perovskites for Lean Methane Combustion: Effect of Synthesis Method. *Advances in Materials Physics and Chemistry*, **8**, 193-215.
https://doi.org/10.4236/ampc.2018.84013

Received: February 28, 2018
Accepted: April 27, 2018
Published: April 30, 2018

Abstract

The effect of the preparation method on the properties of $LaMnO_3$ and $La_{0.8}Sr_{0.2}MnO_3$ perovskite was studied. Materials were prepared by four methods: sol-gel, chemical combustion, solvothermal and spray pyrolysis and characterized. The effect of the synthesis method on the texture, acid-base character of the surface, reducibility with hydrogen, oxygen desorption, surface composition and catalytic activity for combustion of lean methane was studied. It was found that synthesis method affects physicochemical properties of obtained materials-solvothermally produced materials exhibit well-developed surface area, presence of reactive oxygen species on surface and high catalytic activity for CH_4 combustion. Generally, $LaMnO_3$ and $La_{0.8}Sr_{0.2}MnO_3$ perovskites show catalytic activity for lean CH_4 combustion comparable or higher than the activity of 0.5 wt.% Pt/Al_2O_3 but lower than 1 wt.% Pd/Al_2O_3.

Keywords

Perovskite, Different Synthesis Method, Lean Methane Combustion, Combustion Rate, Ventilation Air Methane

1. Introduction

Huge amounts of methane are emitted into atmosphere every year from numerous sources like coal mines, animal waste or landfill. Concentration of methane in the atmosphere has been increasing strongly since beginning of XX century. Methane is a greenhouse gas showing 23 times higher global-warming

potential than CO_2 [1]. Emission of methane creates not only threat to the environment but also it is a waste of energy. Ventilation air methane (VAM) represents the largest part of methane emissions from coal mines; in addition concentration of methane in VAM is low and variable. Annually, up to 350 bln m^3 of methane is released from Polish coal mines and only a part of this gas is used, the majority goes into the atmosphere as VAM with a methane concentration of 0.1% - 1.0% [2]. Conventional flame burners possess insufficient efficiency to oxidize diluted methane in VAM and catalytic oxidation is often proposed for this purpose. However methane is more difficult to oxidize than most of the other hydrocarbons. Catalytic oxidation of methane needs higher temperature than in the case of VOC oxidation therefore not only catalyst activity but also its thermal stability is a crucial problem. Various catalytic systems were proposed for methane oxidation. Noble metals are the most active catalysts however they are susceptible to sintering and expensive as well [3] [4]. Metal oxides seem to be more suitable for such applications than noble metals because they combine low volatility and reactivity with relatively high activity in oxidation reactions and low price [5].

Crystal structure of ABO_3 mixed metal oxides with the perovskite like structure is very flexible towards substitutions and thus allows modifying their physicochemical properties including catalytic activity. Perovskites have been the subject of many studies regarding use their as high-temperature oxidation catalysts [5] [6]. Among different perovskite compositions studied as catalysts of methane oxidation, $LaMnO_3$ appeared to be especially effective in this reaction [7]. Catalytic performances of perovskites are strongly affected by the mobility of oxygen species [8] [9] [10]. Simultaneously, it is commonly known that the method of synthesis strongly affects catalytic performance of the perovskite-type oxides [11] [12]. The amorphous citrate method belongs to the most commonly used in the perovskites synthesis; it is simple and enables one to obtain perovskites at relatively low temperatures. L. Marchetti and L. Forni [6] have found that specific activity of La-Ma based perovskites prepared by amorphous citrate complex method decreases monotonically with increasing temperature of maximum of TPD-O_2 desorption peak. They also stated that two kinds of perovskite related oxygen are active in methane combustion: adsorbed oxygen species active at low temperatures and lattice oxygen species active at high temperatures [6]. In comparison, flame-spray pyrolysis leads to perovskites with small crystal size and good thermal stability, but the apparatus needed for synthesis is rather complicated. Catalytic activity of perovskites prepared by this method increase with increasing surface area of material [13].

The most important advantages of the solvothermal method of perovskites synthesis are high quality and purity of the products, short reaction time, low dispersion of grain size and no need to final high temperature calcination of product. The main disadvantage is a relatively high cost. F. Teng *et al.* [14] prepared $La_{0.5}Sr_{0.5}MnO_3$ single-crystal cubes and nanoparticles by hydrothermal and

citrate routes, respectively. They have found that after running at 600˚C for 48 h under reaction conditions, surface area of nanoparticles decreased significantly while cubes nearly maintained their surface area and latter show higher activity for methane combustion than nanoparticles [14].

H. Najjar *et al.* [15] using $LaMnO_3$ prepared by chemical combustion for methane combustion found that the highest catalytic activity shows perovskite obtained with the use of fuel described by glycine-to-nitrate ratio of 0.8. This material exhibits the highest superficial concentration of manganese and the highest amount of active oxygen [15].

A number of other methods of perovskites synthesis has been elaborated, these ones mentioned above belongs to the most commonly used. Ch. Zhang *et al.* [16] studied the effect of the method of $LaMnO_3$ synthesis on its catalytic performance for toluene oxidation. They have prepared this material by citrate sol–gel, glycine combustion and co-precipitation. Perovskite prepared by sol-gel method showed the best catalytic activity and durability. This superior catalytic performance was attributed to its higher specific surface area, better low temperature reducibility and more available surface adsorbed oxygen species. The lowest apparent activation energy of this material was in good agreement with its high catalytic activity for toluene oxidation [16].

This paper reports results of comparative investigation of the physicochemical properties of the $LaMnO_3$ and $La_{0.8}Sr_{0.2}MnO_3$ perovskites prepared by different synthesis routes (spray pyrolysis, sol-gel with citric acid, solvothermal and chemical combustion). The goal of the work was to determine effect of the synthesis procedure on the properties and catalytic performances for lean methane oxidation of the $LaMnO_3$ and $La_{0.8}Sr_{0.2}MnO_3$ perovskites.

2. Experimental

2.1. Samples Preparation

Mixed oxides with general formula $LaMnO_3$ (LM) and $La_{0.8}Sr_{0.2}MnO_3$ (LSM) were prepared using following methods of synthesis: sol-gel (SG), chemical combustion (CC), microwave-assisted solvothermal (MS) and spray-pyrolysis (SP) method. The details of preparation are as follows:

Sol-gel method: Nitrates of corresponding metals (molar ratio 1:1 for LM and 0.8:0.2:1 for LSM) were dissolved in demineralised water acidified by HNO_3. To the homogeneous solution citric acid was added (molar ratio metal/citric acid = 1:2.5). The solution was then evaporated at 80˚C to produce viscous syrup, which was dried for 24 h at 110˚C and then grinded and calcined by using 3 steps during calcination: 4 h/180˚C, 1 h/300˚C and 4 h/750˚C.

Chemical combustion method: This method is based on the highly exothermic reaction between the metal salts and organic fuel—here glucose was used. It is self-sufficient energy synthesis because the heat required to the synthesis are provided by the reaction itself. Nitrates of corresponding metals (in molar ratio 1:1 for LM and 0.8:0.2:1 for LSM) were dissolved in a small amount of demine-

ralized water. Glucose was then added to the obtained solution, a mass of glucose was equal to the mass of all salts. The resulting solution was concentrated in a rotary evaporator at 80˚C to produce viscous syrup, which was dried for 24 h at 110˚C and then calcined for 6 h at 750˚C.

Microwave-assisted solvothermal method: nitrates of corresponding metals were dissolved in ethylene glycol and reacted in a teflon melting pot in an autoclave (90 min, 200˚C, 40 bar) under microwave heating. The resulting suspensions were centrifuged, washed with acetone, dried (24 h/110˚C) and then calcined (4 h/750˚C, 10˚C/min).

Spray-pyrolysis method: The hydrated nitrates of corresponding metal were dissolved in distilled water (0.45 mol/dm^3). The resulting solution was filtered and then sequentially pumped into the chamber system by a peristaltic pump. Powder synthesis reaction was carried out under the following conditions: solution flow rate 30 ml/min with performance of 0.1137 dm^3/min, pressure 13.8 bar, the temperature 500˚C. The resulting powder was filtered through a cotton filter, dried 24 h/110˚C and then calcined 4 h at 750˚C (10˚C/min).

2.2. Characterization Techniques

The prepared mixed oxides were characterized by means of: X-ray diffraction (XRD), specific surface area determination, scanning electron microscopy (SEM), temperature programmed reduction with hydrogen (TPR H_2), decomposition of cyclohexanol (CHOL), temperature programmed desorption of CO_2 (TPD CO_2), temperature programmed desorption of oxygen (TPD O_2), X-ray photoelectron spectroscopy (XPS) and tests of catalytic activity for lean methane combustion.

By using an X'Pert Powder Diffractometer (PANalytical), working in the reflection geometry and using CuKα radiation (λ = 1.54056 Å) X-ray diffraction (XRD) patterns were recorded. The data were collected in the 2Θ range 10˚ - 80˚ (step of 0.026˚). The fitting of the diffraction peaks was done by WinPLOTR programme [17]. The lattice parameters were calculated by DICVOL programme implemented in FullProf Suite package. The average size of crystallites was calculated based on Scherrer method (for line at about 2Θ ≈ 46˚ and with parameter K = 1), as described in [18] [19].

The specific surface area was determined by the BET method (Brunauer-Emmett-Teller) using the Quantachrome Autosorb-1C. The BET surface was calculated from the N_2 adsorption isotherm at −196˚C (77 K), in the range of relative pressures p/p_o from 0.05 to 0.35. Prior to the measurements, samples were degassed at 200˚C for 2 h to remove adsorbed contaminants such as water.

The morphology of the samples was determined using a scanning electron microscope SEM/Hitachi S-3400N while elemental composition of selected sites on their surface were determined using energy-dispersive X-ray spectroscopy (EDS).

The susceptibility of the prepared materials to reduction was determined by

temperature programmed reduction with hydrogen (TPR H_2). TPR H_2 measurements were made using Pulse ChemiSorb 2705 apparatus. The 50 mg of sample was placed in a U-tube quartz reactor and then heated to 900˚C (heating rate of 10˚C/min). Through the catalyst bed was passed the mixture of 5% vol. of H_2 in Ar (30 ml/min). Hydrogen consumption was measured by thermal conductivity detector (TCD).

The share of acid-base centers on the surface of tested materials were determined by decomposition of cyclohexanol (CHOL), determining the selectivity of the conversion of this compound to dehydration and dehydrogenation products. The dehydration of CHOL occurs on acid sites and leads to cyclohexene (CHEN), while the dehydrogenation of CHOL, leading to cyclohexanone (CHON), requires the interaction both acid and basic centers. It is accepted, that selectivity of CHOL decomposition to CHEN (S_{CHEN}) is a direct measure of acidic character of material surface, while the CHON/CHEN selectivities ratio (S_{CHON}/S_{CHEN}) gives information about basic nature of surface [1]. The 0.1 g of sample was diluted within silicon carbide to a volume of 1 cm^3 and then placed in a quartz reactor between two layers of quartz wool. The reactor was moved into the furnace chamber and heated to 300˚C with a rate of 15˚C/min in a carrier gas stream (N_2, 10 dm^3/h). Then the reactor was purged with nitrogen saturated by cyclohexanol (10 dm^3/h). Products of CHOL decomposition were analyzed by gas chromatograph equipped with flame ionization detector (FID).

Measurements of temperature programmed desorption of oxygen (TPD O_2) was performed by using a Micromeritics AutoChem II 2920 analyzer equipped with a TCD detector. The 100 mg of samples were placed in a quartz reactor, then moved into the furnace chamber and heated in a stream of O_2 from 25˚C to 500˚C for 1 h. The reactor was cooled to 40˚C and a stream of inert gas was passed through the catalyst bed (He, 30 ml/min) for 0.5h. Next the samples were heated, in the stream of He, from 40˚C to 950˚C (10˚C/min.). The content of O_2 in the effluent gas was determined by a mass spectrometer (OmniStar QMS 200, Pfeiffer Vacuum) while monitoring the m/e signal 32 (O_2).

The surface composition of the prepared materials was determined by X-ray photoelectron spectroscopy (XPS), using a SPECS XPS/UHV system equipped with a PHOIBOS 100 spectrometer. The X-ray source was an Mg anode operating at 100 W (survey scan) and 250 W (high resolution spectra), Ar(+) sputtering (90", 7 μA/cm^2, 3 keV). The analyzer mode was set at constant analyzer energy mode. Sample charging was compensated using an electron flood at 0.5 mA current and 0.1 eV energy. The C1s peak of the contamination carbon, at 284.6 eV, was taken as reference. The detection angle was normal to the surface. The spectra were collected and processed using SPECLAB software. Non-linear least-squares fitting algorithm was performed using peaks with a mix of Gaussian-Lorenzian shape and a Shirley baseline.

Catalytic activity in lean CH_4 combustion was tested in a continuous-flow fixed bed quartz reactor, placed in a tube furnace with a single heating zone. The

temperature was measured with a thermocouple positioned a few millimeters below the top of the catalyst bed. Temperature of reactor was raised (5˚C/min) from 25˚C to 550˚C. The 200 mg of catalyst diluted in 200 mg of SiC was loaded into a tubular quartz reactor on a thin layer of quartz wool. The reagents mixture (0.6 vol% of CH_4 and 21 vol% of O_2 in argon) was fed to the reactor with flow rate corresponding to GHSV = 40,000 h^{-1}. The gas mixture flow rate was 8 dm^3/h and was adjusted by mass flow controllers. The reaction products were analyzed by GC (PERKIN ELMER Autosystem XL with capillary column (30 m × 0.25 mm × 0.25 μm), equipped with FID detector. The reaction rate per m^2 (r_{SSA}) of the catalyst was calculated using formula:

$$r_{SSA} = \frac{F_{CH_4}}{SSA} \times \alpha \times 10^6$$

where F_{CH_4} is the flow rate of methane ($mol \cdot s^{-1}$), α is methane conversion and *SSA* is specific surface area.

3. Results and Discussion

Regardless of the method of synthesis used, the X-ray diffraction patterns of all materials are similar to each other and characteristic for perovskite-like structure (PDF card No. 00-032-0484 for LM and PDF card No. 00-040-1100 for LSM), as can be seen from **Figure 1**. All LM prepared materials crystallized in a trigonal system in crystallographic space group R-3c (the cell parameters of a = b ~ 5.5 Å) (**Table 1**). The LSM samples crystallized in regular system in the space group Pm-3m (cell parameters a = b = c ~ 3.9 Å), except of LSM-CC, which crystallized in a trigonal system (**Table 1**). Diffractograms of synthesized materials show no phase contaminants, only the XRD pattern of LSM-SP, besides reflections coming from $La_{0.8}Sr_{0.2}MnO_3$, shows a weak lines characteristic for La_2O_3 (2Θ = 30, 46,

Table 1. The average size of crystallites of dominant phase and unit cell parameters of LM and LSM perovskites prepared by different methods.

Method of synthesis	Sample	Crystal. System	Space group	a*, **, Å	c, Å	γ***, °	Average size of crystal., nm	
							from XRD	from SSA
SG	LM	Trig.	R-3c	5.506(3)	13.335(7)	120	37	83
	LSM	Reg.	Pm-3m	3.878(2)	-	90	25	34
CC	LM	Trig.	R-3c	5.504(4)	13.332(13)	120	32	61
	LSM	Trig.	R-3c	5.503(2)	13.360(5)	120	36	51
MS	LM	Trig.	R-3c	5.503(3)	13.321(8)	120	25	57
	LSM	Reg.	Pm-3m	3.881(2)	-	90	22	48
SP	LM	Trig.	R-3c	5.506(2)	13.321(5)	120	44	152
	LSM	Reg.	Pm-3m	3.855(2)	-	90	16	83

* - For trigonal system a = b ≠ c ** - For regular system a = b = c *** - The angle between the axes.

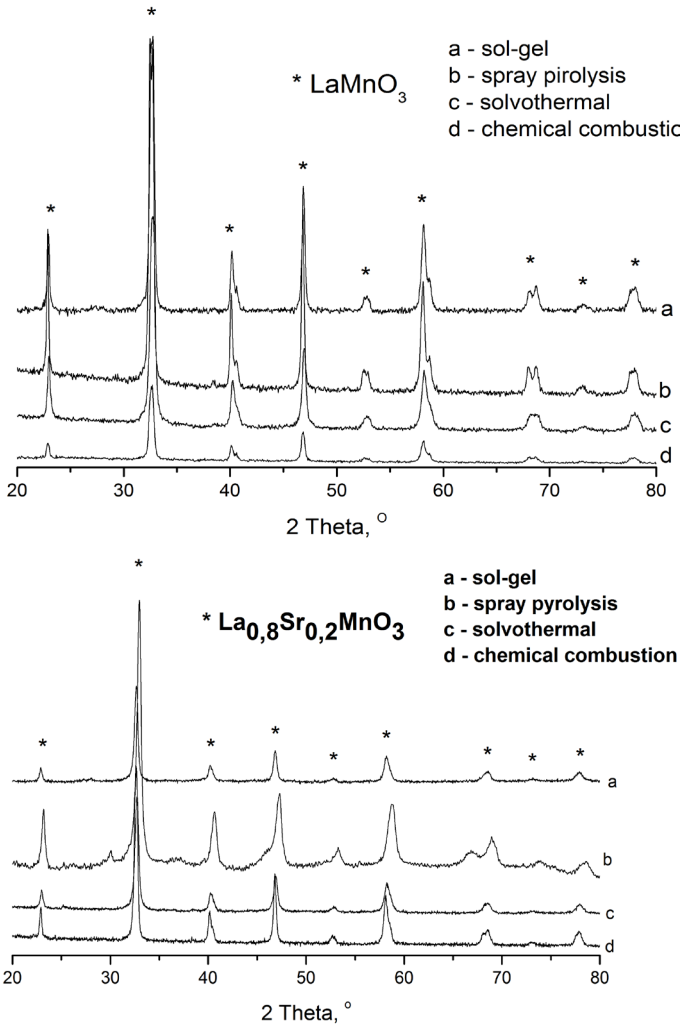

Figure 1. X-ray diffraction patterns of LM (a) and LSM (b) perovskites.

67˚, PDF card No. 00-005-0602) (**Figure 1(b)**). X-ray diffraction patterns of LM-MS differs from XRD patterns of LSM-MS. The presence of strontium results in a less intense peaks, which translates into smaller particle size. An average size of crystallites are gathered in the **Table 1** and were determined from XRD and SSA. The LM and LSM prepared by sol-gel, chemical combustion and solvothermal method show a similar crystallites size, taking into account the crystallites from XRD, comprising in the range of 22 - 37 nm. The average size of crystallites of materials prepared by spray pyrolysis do not lie within this range and amounts to 16 nm for LSM and 44 nm for LM (**Table 1**). An average crystal sizes were also calculated based on the values of specific surface area and density of LM (LSM) equal to 6.57 g/cm^3 (**Table 1**). Estimated in this way corresponding values of crystal size are bigger than those calculated with Scherrer equation. It means that part of the crystallites surface is inaccessible for adsorption/reaction.

All studied LM and LSM mixed oxides show relatively low specific surface area (**Table 2**) that depends on the method of their synthesis. Among the LM samples, the largest SSA shows the one synthesized *via* solvothermal route, while

Table 2. Specific surface area and results of CHOL decomposition.

Method of synthesis	Sample	S_{BET}, m^2/g	Decomposition of cyclohexanol			
			Conversion of CHOL, %	*Selectivity to CHEN, %*	*Selectivity to CHON, %*	*Y*
SG	LM	11	9	71	29	0.4
	LSM	27	9	51	49	1.0
CC	LM	15	15	63	37	0.6
	LSM	18	12	80	20	0.3
MS	LM	16	10	63	37	0.6
	LSM	19	16	71	29	0.4
SP	LM	6	8	84	16	0.2
	LSM	11	21	88	12	0.1

among the LSM materials, this one obtained by the sol-gel method. Both samples prepared by spray pyrolysis are characterized by the smallest value of SSA. The partial substitution of lanthanum by strontium, for all of used methods of synthesis, leads to a material with a higher specific surface area.

Acid-base properties of the studied materials were determined by the method of cyclohexanol (CHOL) decomposition. On the surface of the mixed metal oxides with perovskite like structure nucleophilic oxide ions O^{2-} are present (basic sites of a Lewis type) [20] and the electrophilic ions O^-, O_2^{2-}, O_2^- [21]. The ratio (selectivity to CHON)/(selectivity to CHEN) denoted here as a Y is considered as a measure of the share of basic centers [22]. Samples LM-CC, LM-MS and LSM-SG show the highest share of basic sites (**Table 2**), respectively 0.6 (LM-CC and LM-MS) and 1.0 (LSM-SG). Acidic sites prevail on the surface of both materials prepared by SP as it is evidenced by the highest value of selectivity to CHEN: 84% for LM and 88% for LSM (**Table 2**).

The morphology of the studied perovskites was characterized by scanning electron microscopy (SEM) technique.

Typical SEM pictures of LM surface are presented in **Figure 2**. According to literature substitution of La by Sr doesn't significantly affects the morphology of the material [23]. The morphology of LM perovskites depends on the method of their synthesis. LM-SG and LM-CC create agglomerates. Material synthesized by CC is more porous and particles are terminated with sharp edges. In contrast, LM-MS consists of fine, solid crystallites with regular shapes, between which free spaces are visible. The morphology of the LM-SP differs markedly from the other materials, because it looks like sintered scales with low porosity without visible crystallites. As it was pointed above, calculated from SSA crystal size of both materials prepared by MS method are bigger than in case of corresponding materials prepared by other methods.

The TPR H_2 profiles of studied materials are shown in **Figure 3** and the temperatures of maximum of hydrogen consumption are summarized in **Table 3**.

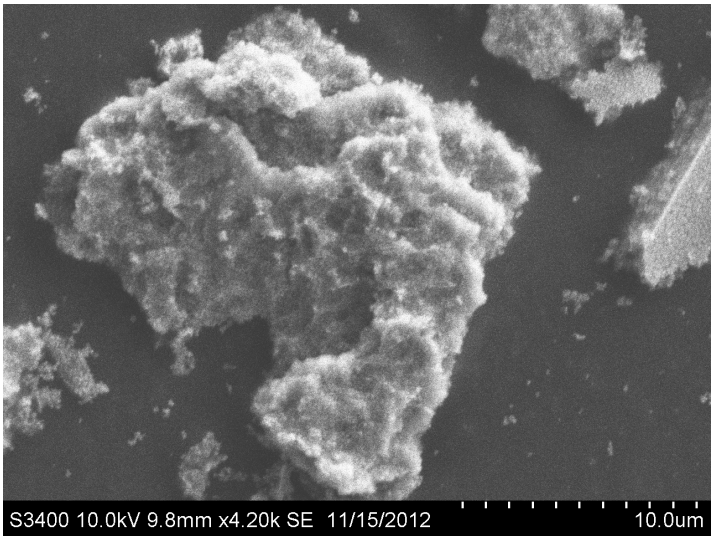
S3400 10.0kV 9.8mm x4.20k SE 11/15/2012
10.0um

(a)

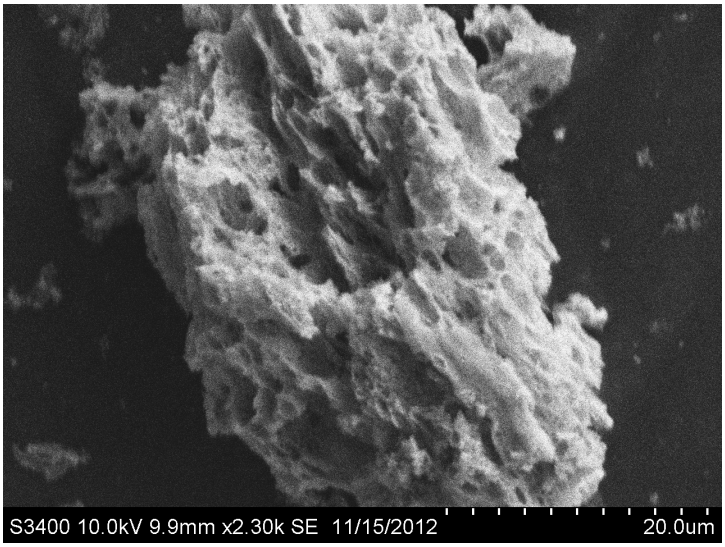
S3400 10.0kV 9.9mm x2.30k SE 11/15/2012
20.0um

(b)

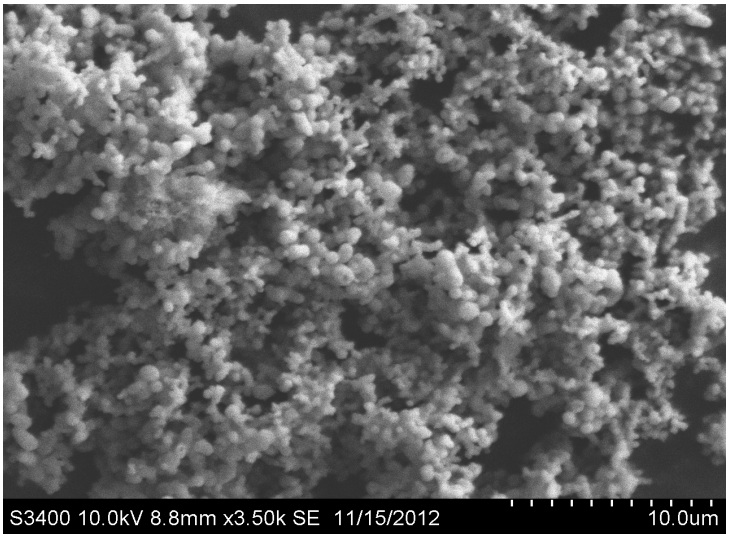
S3400 10.0kV 8.8mm x3.50k SE 11/15/2012
10.0um

(c)

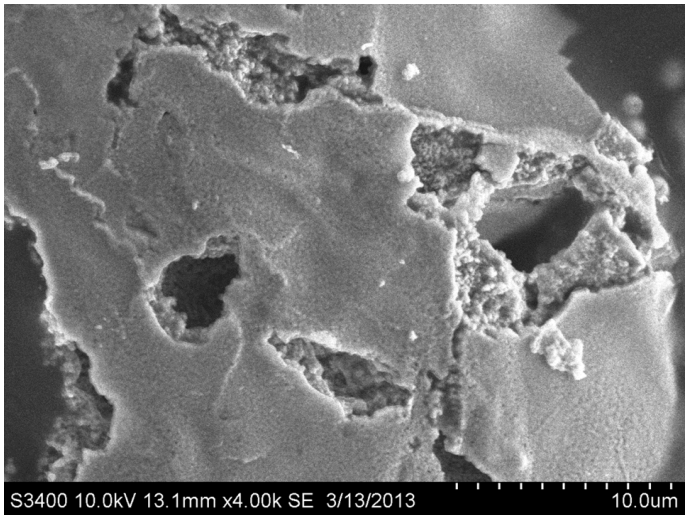

(d)

Figure 2. SEM images of the LM perovskites prepared by different methods: (a) LM-SG; (b) LM-CC; (c) LM-MS; (d) LM-SP.

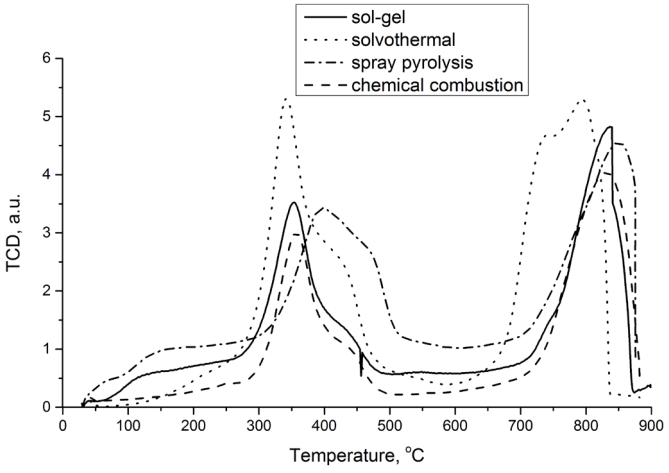

(a)

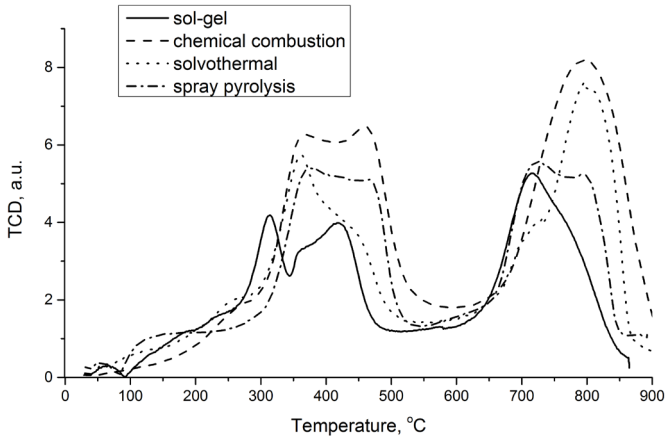

(b)

Figure 3. TPR H_2 profiles of: (a) LM and (b) LSM prepared by different method.

Table 3. Results of TPR H2—temperatures of maximum of hydrogen consumption.

	SG		*CC*		*MS*		*SP*	
	LM	*LSM*	*LM*	*LSM*	*LM*	*LSM*	*LM*	*LSM*
T_I, °C	352	314	357	364	343	361	397	464
T_{II}, °C	835	716	830	794	792	794	849	726

The TPR H_2 profiles of Mn-containing materials show two intensive peaks of hydrogen consumption (**Figure 3**). First peak, with maximum of hydrogen consumption at the temperature range 343˚C - 459˚C (T_I), represents the reduction of Mn^{4+} to Mn^{3+} while the second one (maximum intensity in the range 716˚C - 849˚C (T_{II})) is ascribed to the reduction of Mn^{3+} to Mn^{2+} [5] [16]. The presence of Mn^{4+} is related to the fact that the Mn^{3+} has a free electron, which making Mn^{3+} ion capable to adsorption of molecular oxygen and its transformation into an electrophilic forms, which are very active in the oxidation reactions [24]:

$$Mn^{3+} + O_2 \rightarrow O_2^- / O^- + Mn^{4+}$$

The shapes of TPR H_2 profiles of all LM and LSM materials are similar, regardless of the method of synthesis. Nevertheless, the influence of the synthesis method on the temperature of maximum of H_2 consumption is observed. The temperatures of reduction T_I and T_{II} of LM perovskites lower in the following order of synthesis method: SP > SG > CC > MS. LM-SP exhibits the highest value of T_I (397˚C) and T_{II} (849˚C) (**Table 3**)—spray pyrolysis leads to a material characterized by a low susceptibility to reduction, what probably results from a significant sintering of this material. On the other hand LM-MS, that exhibits the smallest size of crystallites, reacts with hydrogen at the lowest temperatures: T_I - 343˚C and T_{II} - 792˚C.

The TPD O_2 profiles of studied materials are shown in **Figure 4**. Amount of oxygen released from them are summarized in **Table 4**. The investigated materials release oxygen in the temperature range 200˚C - 900˚C. TPD O_2 profiles of all samples possess similar shape and show three regions of oxygen desorption. Based on the data presented in **Table 4** and **Figure 4** one can conclude that synthesis method affects the amount of oxygen desorbed from the surface of corresponding material. The highest amount of oxygen (per gram) release materials prepared by MS method, while the lowest these ones prepared by SP; these differences are smaller when amount of desorbed oxygen is calculated per m^2 of SSA. The amount of oxygen released from the surface of studied here materials are close to the values reported in the literature. M. Alifanti *et al.* [25] reported 267.3 μmol O_2/g while Rosso *et al.* found 263 μmol O_2/g [26] desorbed from the surface of $LaMnO_3$ prepared respectively by citrate and the modified citrate method. Other researchers reported the 262.3 μmol O_2/g and 437.8 μmol O_2/g (total amount) desorbed from $LaMnO_3$ and $La_{0.6}Sr_{0.4}MnO_3$ prepared by citric acid complexing coupled with hydrothermal method [27].

Depending on the desorption temperature, three forms of oxygen are distinguished on the perovskite surface [28]. Desorption at temperatures up to ca

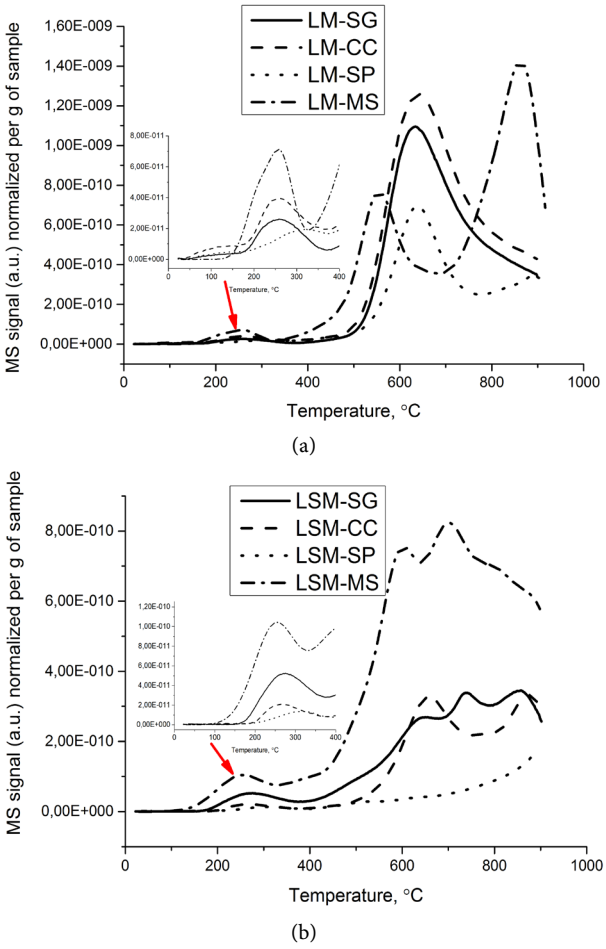

Figure 4. TPD O_2 profiles of LM perovskites (a) and LSM (b) perovskites.

Table 4. Results of TPD O2 experiments.

sample	Amount of oxygen desorbed, μmol O_2/g (μmol O_2/m^2)			
	α_1	α_2	β	Total
LM-SG	7 (0.6)	427 (39)	-	434 (39)
LSM-SG	14 (0.5)	130 (5)	62 (2)	206 (8)
LM-CC	14 (1)	511 (34)	-	525 (35)
LSM-CC	5 (0.3)	97 (5)	63 (4)	165 (9)
LM-MS	28 (2)	197 (12)	341 (21)	566 (35)
LSM-MS	35 (2)	346 (18)	146 (8)	527 (28)
LM-SP	6 (1)	105 (18)	61 (10)	172 (29)
LSM-SP	5 (0.5)	48 (4)	-	53 (5)

400˚C is associated with the surface oxygens, described as α_1-oxygen, which are commonly attributed to weakly chemisorbed oxygen molecules upon surface-oxygen vacancies. The oxygen described as α_2 is a near-surface oxygen associated with lattice defects such as dislocations and grains frontiers. This form of

oxygen desorbs at temperatures from the range 400˚C - 700˚C and is completely associated with the oxidation of diluted methane, together with α_1-oxygen [29]. These both kinds of oxygen are designed as α-O_2 that generally desorbs below 700˚C. It is known, that the desorption temperature of α-oxygen strongly depends on the calcination temperature and it is supposed that at the temperature of desorption, α-oxygen species (eg. O_2^-) dissociate into atomic species [29]. Oxygen that desorbs above ca 750˚C is denoted as $\beta$and generally is linked with the lattice oxygen. This oxygen species can be directly associated with the reduction of B-site cation – here reduction of Mn^{4+} [28].

All studied LM and LSM perovskites desorb α_1, α_2 and βoxygen (**Figure 4**). One can state the effect of synthesis method on the amount of various forms of desorbed oxygen. As it is seen on **Figure 4**, α-oxygen desorbs at wide range of temperatures. The LM perovskites evolve a small amount of oxygen at temperature range 180˚C - 350˚C (maximum of desorption around 250˚C); much higher amount of O_2 is desorbed from these materials at temperatures above 400˚C with maximum of desorption depending on the sample: at 555 and 862˚C (LM-MS); 632˚C (LM-SG) 634˚C (LM-SP) and 645˚C (LM-CC). Only for LM-MS two peaks of desorption are observed >400˚C. Partial substitution of La by Sr greatly lowers amount of oxygen desorbed from corresponding sample with the exception of material prepared by solvothermal method (LSM-MS) for which depletion of the amount of desorbing oxygen is negligible. Similar effect of Sr incorporation was reported by S. Ponce *et al.* [27] and D. M. A. Melo *et al.* [30] who investigated the $La_{1-x}Sr_xMnO_3$ perovskites synthesized by: amorphous citrate decomposition [27] and by Pechini method [30] and showed that the amount of O_2 desorbed from its surface decreases with increasing Sr content. The LSM perovskites desorb oxygen in a wider temperature range than LM ones. The materials prepared by solvothermal method desorb the most of oxygen per gram, while the samples synthesized using spray pyrolysis method the least of all. The amount of α-oxygen (per gram) released by the LM perovskites decreases in the order: CC > SG > MS > SP. The sequence for the amount of α-oxygen per unit surface area is as follows: SG > CC > SP > MS. The samples prepared by MS method desorb much more β-oxygen (per gram and per m^2 of sample) than these ones prepared by other methods.

The onset temperature of α_1-oxygen desorption from LM perovskites increased with the order MS < CC < SG < SP while in the case of materials substituted by strontium the order is following: MS < SG < CC < SP (**Figure 5**).

Oxides of lanthanum and strontium are very reactive and in contact with the atmospheric air form surface carbonates, hence on the surface of materials large amount of carbon are present. The surface of all the studied materials is enriched with La (**Table 5**) with respect to the theoretical value. It can be explained by the fact that the surface of $LaMnO_3$ may exhibit one of the two ends with opposite polarity and charge: +1e (terminated LaO) and −1e (terminated MnO_2). Due to the enrichment of surface of materials with La, it is likely that they have LaO

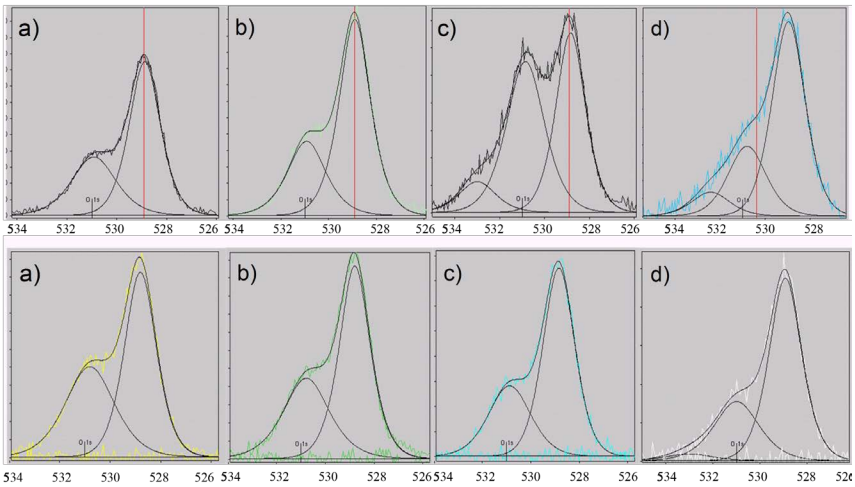

Figure 5. XPS patterns O 1s (after deconvolution) LM (at the top) i L_8S_2M (at the bottom) prepared by method: (a); SG; (b) CC; (c) MS; (d) SP.

Table 5. The surface composition of the studied materials

Method of synthesis		SG		CC		MS		SP	
Sample		LM	LSM	LM	LSM	LM	LSM	LM	LSM
La, % at.		20.8	12.7	18.9	16.4	19.3	17.4	18.5	15.8
Mn, % at.		10.0	12.8	11.3	11.9	10.2	11.8	12.0	13.4
share of Mn^{4+}/Mn, %		25.4	25.8	23.9	24.1	14.2	41.4	17.7	21.7
Sr, % at.		-	2.8	-	2.6	-	2.3	-	4.3
O, % at.		56.6	59.0	59.2	57.2	58.7	56.5	56.4	58.9
C, % at.		12.6	12.7	10.6	11.9	11.8	12.0	13.1	7.6
La:Mn	T	1:1	0.8:1	1:1	0.8:1	1:1	0.8:1	1:1	0.8:1
	E	2.1:1	1:1	1.7:1	1.4:1	1.9:1	1.5:1	1.5:1	1.2:1
La:Sr	T	-	4:1	-	4:1	-	4:1	-	4:1
	E	-	4.5:1	-	6.3:1	-	7.6:1	-	3.7:1

T—theoretical ratio; E—experimental ratio.

termination. The surface characterized by such termination adsorbs oxygen atoms in the place of bridge La-La, which results in the more energetically favorable configuration of the material [31] [32]. Partial substitution of La by Sr changes composition of the surface: the content of La decreases while Mn increases (Table 5). The effect of the synthesis method on the surface composition of materials is observed, as evidenced by the differences in experimental ratio of La:Mn, La:Sr. The content of strontium on the surface of the material increases in the following order of synthesis methods: MS < CC < SG < SP. The theoretical content of Sr in the LSM is 7.42% by weight. LSM perovskites were dissolved in nitric acid and the content of strontium was determined by ICP method. It turned out that LSM prepared by both SG and CC methods show close to ex-

pected content of strontium while samples prepared by MS and SP contain less strontium than it comes from stoichiometry, respectively (wt.%): 6.12 and 6.95. Strontium nitrate used as one of the precursors in the LSM synthesis is relatively easily volatile (melting point/boiling point respectively 570/645˚C) [33], what may explain lower content of Sr in the sample synthesized at high temperature (SP method). Good solubility of $Sr(NO_3)_2$ in ethylene glycol probably is a reason of lower content of Sr in the LSM-MS sample. Surface of LSM-MS shows the lowest Sr content what is consistent with the ICP analysis results. In turn, the highest content of Sr on the surface of LSM-SP probably results from the specificity of spray pyrolysis causing the accumulation of the more volatile component on the surface of the grain.

S. Ponce *et al.* [27] reported that the stability of Mn^{4+} ions is an important parameter which increases the catalytic activity of the materials. A measure of stability is the fact that, despite the thermal treatment at high temperatures and under high vacuum, Mn^{4+} ions are still present on the surface of material. They have shown that with increasing share of Mn^{4+} on the $La_{1-x}Sr_xMnO_3$ (x = 0 - 0.5) surface its activity in the methane combustion also increases. As a result of the partial substitution of La by Sr, nonstoichiometric mixed oxides $La_{1-x}Sr_xMnO_{3-\delta}$ is formed and oxidation of Mn^{3+} to Mn^{4+} takes place in order to compensate the charge [27] [34]. Similarly B.M. Nagabhushana [35] reported, that Mn^{4+} content increases with increase of Sr content. LSM materials studied in this work are characterized by higher share of Mn^{4+} on the surface than corresponding LM ones. Among LSM materials the largest share of Mn^{4+} on the surface was found for LSM-MS and LSM-SG, while the lowest values could be found in LSM-SP. When La^{3+} is partially substituted by Sr^{2+}, the charge is compensated by the oxidation of Mn^{3+} to Mn^{4+} and/or formation of vacancies [36]. N. Yamazoe and Y. Teraoka observed decreasing of the high temperature oxygen desorption (β-oxygen) with increasing degree of Sr substitution. They explained this observation by the intrinsic nature of Mn ions: in order to mitigate the static Jahn-Teller distortion, $LaMnO_3$ has to have a certain number of cation vacancies, accompanied with formation of Mn^{4+} ions and oxygen-excess nonstoichiometry ($LaMnO_{3+\delta}$) [37]. In our study we observed that substitution of La by Sr only slightly increase the share of Mn^{4+} on the surface of materials prepared by SG and CC methods while this effect is greater for LSM samples prepared by MS and SP methods. Since the samples prepared by both latter methods contain less Sr than it is required by the stoichiometry, for charge compensation part of Mn^{3+} passes to Mn^{4+} oxidation state. For these reasons there is only little space for introducing oxygen vacancies in the lattice of these materials because electroneutrality can be ensured by change Mn^{3+} to Mn^{4+}. Oxygen species desorbing at high temperatures (β-O_2) may be formulated according following reaction [38]: $4Mn^{4+} + 2O^{2-}(\square) \rightarrow 4Mn^{3+} + O_2$ where ($\square$) is a cation vacancies. Taking into account the high value of Mn^{4+}/Mn ratio (**Table 6**) on the surface of LSM-MS, it is clear why concentration of β-O_2 on the surface of this material is distinctly higher than in case of other studied here perovskites.

Table 6. The share of oxygen forms on the surface, % at.

Form of oxygen	SG		CC		MS		SP	
	LM	LSM	LM	LSM	LM	LSM	LM	LSM
O^{2-}, % at.	64.9	57.1	66.2	61.7	43.6	67.0	64.6	66.7
OH^- and CO_3^{2-}, % at.	35.1	42.9	33.8	38.3	47.1	33.0	26.4	29.9
H_2O, % at.	-	-	-	-	9.3	-	9.0	3.4
O_{lat}/O_{ads}	1.85	1.33	1.96	1.61	0.93	2.03	2.45	2.23

In addition, as it was shown above, the morphological and textural properties of studied perovskites are strongly affected by the method of synthesis. S. Royer *et al.* have shown that amounts of desorbed different *α*-oxygens is mainly dependent on the specific surface area of the material [39]. All these factors make the TPD-O_2 profiles of the investigated materials differ significantly.

Three forms of oxygen are present (**Table 6**, **Figure 5**) on the surface of studied perovskites: lattice oxygen O^{2-} (BE about 528.8 eV), adsorbed oxygen species like hydroxyls and carbonate OH^- / CO_3^{2-} (BE about 530.9 eV) and H_2O (BE about 533.0 eV) [40] [41]. Generally, the shifts of O 1s BE resulted from the synthesis method or substitution by Sr are insignificant.

However, both the method of synthesis and substitution by Sr exert a significant influence on the share of oxygen forms on the surface of these materials (**Table 6**). Lattice oxygen is the main form of oxygen species on the surface and it is confirmed by value of O_{lat}/O_{ads} ratio, which amounts in case of LM: 0.93; 1.85; 1.96; 2.45 respectively for MS, SG, CC and SP synthesis method and in case of LSM: 1.33; 1.61; 2.03; 2.23 respectively for SG, CC, MS and SP method. The high share of O^{2-} is observed on the surface of both samples prepared by SP method. Partial substitution of La by Sr in samples prepared by SG and CC method, lowers the share of O^{2-}, while in the case of MS and SP method the effect is opposite. Higher share of lattice oxygen on the surface of the latter two materials, probably results from the presence of cationic vacancies (lower than stoichiometric content of Sr), what in turn limits the possibility of creating anionic vacancies on the surface of both latter materials.

The results of lean methane combustion on studied LM and LSM perovskites are reported in **Figure 6**, **Table 7** and **Table 8**. Activity (temperature of 10%, 50% and 90% conversion of methane) of studied catalysts was compared with activity of 0.5% Pt/Al_2O_3 and 1% Pd/AlO_3 and presented in **Table 7**.

All prepared perovskites exhibit catalytic activity in lean methane combustion. Depending on the method of synthesis, the temperature of 10%, 50% and 90% conversion of CH_4 differs significantly. The highest activity exhibits LM-MS, it enables the total methane conversion at 451˚C. Slightly less active is LSM-CC ($T_{100\%}$ = 455˚C). The catalytic activity of 0.5% Pt/Al_2O_3 is low and comparable with the activity of both samples prepared by spray pyrolysis method while 1% Pd/Al_2O_3 is significantly more active than all other studied materials. The partial

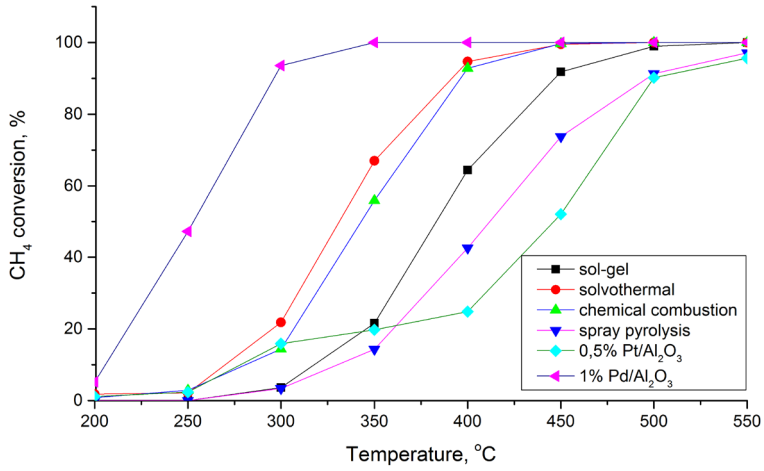

(a)

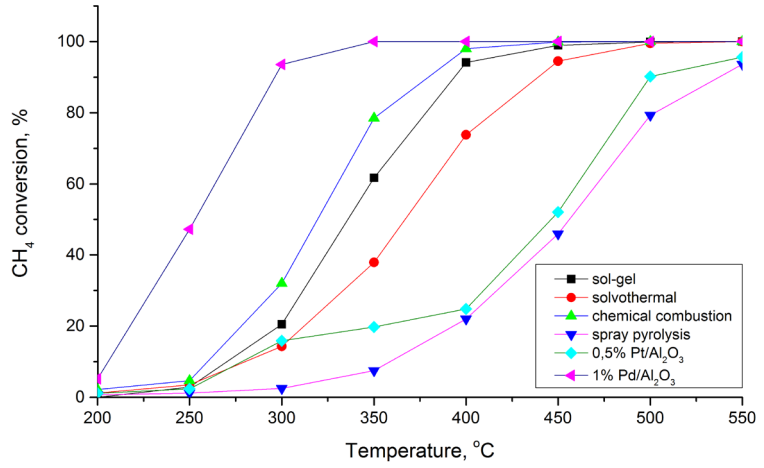

(b)

Figure 6. Conversion of methane on studied LM (a) and LSM (b) perovskites vs temperature

Table 7. Results of catalytic activity tests—temperatures of 10%, 50% and 90% of methane conversion

	SG		CC		MS		SP		0.5% Pt/Al_2O_3	1% Pd/Al_2O_3
	LM	LSM	LM	LSM	LM	LSM	LM	LSM		
$T_{10\%}$,	313	270	237	266	269	280	330	359	278	205
$T_{50\%}$,	379	333	351	329	331	363	410	452	446	252
$T_{90\%}$,	443	397	375	389	392	439	496	537	499	296

substitution of 20% at. of La by Sr in the structure of LM perovskite decreases its activity for combustion of lean methane—only LSM-SG has higher activity than LM-SG.

It seems, that the high catalytic activity of LM samples prepared by MS and CC methods may be explained by their ability to release large amounts of *α* oxygen at relatively low temperatures (Table 4, Figure 4). It is suggested, that these

Table 8. Rates of methane combustion $\times 10^3$, μmol/(s·m^2).

Method	Sample	Temperature, °C		
		300	350	400
SG	LM	0.4	2.0	5.4
	LSM	0.7	2.0	3.1
CC	LM	0.9	3.3	5.5
	LSM	1.2	3.4	4.7
MS	LM	1.2	3.7	5.3
	LSM	0.7	1.8	3.5
SP	LM	0.5	2.1	6.3
	LSM	0.2	0.6	1.8

form of oxygen species are responsible for the oxidation of methane [30]. LM-SP released comparable amount of α_1 and α_2 oxygen (per surface unit) however but at higher temperatures than perovskites prepared by others methods. Apart of this, LM-SP exhibits the value of SSA among LM materials. Both factors make that among studied LM perovskites this one prepared by SP shows the lowest activity in the combustion of diluted methane. The rate of oxidation of methane (per m^2) on the LM perovskites (**Table 8**) increases in the same order (SP < SG < CC < MS) as availability (temperature onset) of α_1-oxygen and does not correlate with either α_1-oxygen concentration (per m^2, **Table 5**) nor O_{lat}/O_{ads} ratio (share of adsorbed oxygen, **Table 6**). Taking into account low concentration of methane in the reaction mixture one can consider, that availability of active oxygen on the surface is at least as important as its amount for the activity of these materials. The confirmation of this conclusion is a linear relationship between rate of methane combustion and temperature of the first maximum of hydrogen consumption for LM perovskites prepared by studied methods (**Figure 7**).

Another factor contributing to higher catalytic activity of LM-MS and LM-CC, is relatively better developed specific surface area of this material, composed of fine crystal particles. In addition, LM-MS reaction with hydrogen starts at the lowest temperature, which suggests the presence of the most reactive oxygen species on the surface.

For the samples containing Sr there are no simple correlations between their properties and the catalytic activity. The highest rate of methane combustion shows material prepared by CC method while the lowest this one prepared by SP method (**Table 8**). At low temperature (300˚C), the rate of methane combustion on the LSM prepared by either by CC or SG is higher than on the corresponding LM. However the rate of combustion on the latter materials increases faster with temperature than on the LSM. The biggest amount (and at the lowest temperature) of α-oxygen desorbs from the surface of LSM-MS, however the reaction rate on this material is lower than on the LSM-CC and comparable to this one on the LSM-SG. Perovskites LSM-MS and LSM-CC show a very similar profile

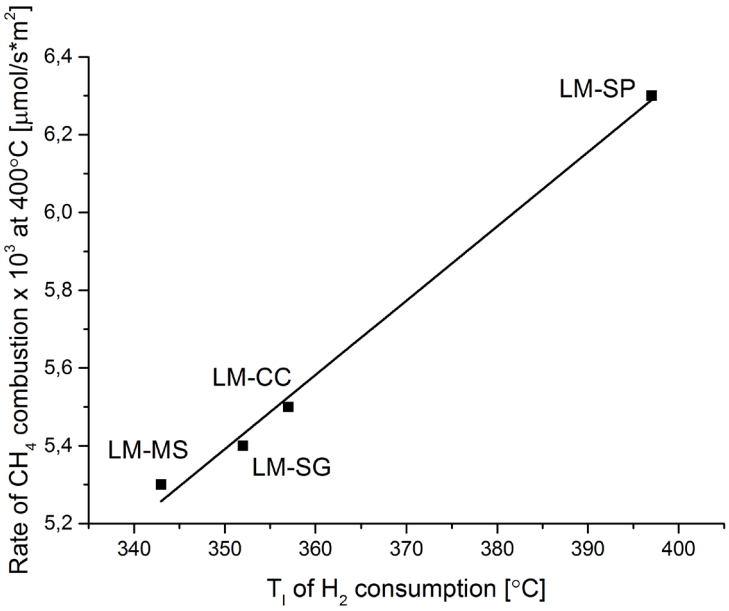

Figure 7. Rate of methane combustion vs temperature of the first maximum of hydrogen consumption for LM perovskites.

TPR-H_2, possess close temperatures T_I and T_{II} and textures. In addition, the LSM-MS desorbs substantially more oxygen (α and β) counterpart prepared by CC. However, the latter perovskite shows a significantly higher catalytic activity than the previous one. The only one which differs these two materials is strontium content—its insufficiency in respect to the stoichiometric in the LSM-MS. Presently we can not explain why the abundance and availability of α-oxygen on the LSM-MS surface is not sufficiently reflected in its activity. Probably β-oxygen present in large amounts on the surface LSM-MS, but desorbing at relatively higher temperatures than in case of other LSM play more important role in methane combustion on this material. In this way one can suppose that unusual catalytic behavior of LSM-MS might be associated with lower than stoichiometric content of Sr resulting in a high share of Mn^{4+}, whereby results of neither TPD-O_2 nor TPR-H_2 can be simply related to the rate of methane oxidation. Relatively low activity of LSM-SP should be attributed to its low SSA and a small amount of adsorbed oxygen species on its surface. High catalytic activity of materials prepared by CC method can be explained on the basis of H. Najjar, H. Batis conclusions who stated that this method of synthesis resulted in a decrease in superficial La/Mn atomic ratio and an increase of relative content of the surface oxygen species what leading to high catalytic activity of corresponding material in the combustion reactions [42]. Our results confirm these findings (**Table 5** and 5): both materials prepared by CC show the low value of experimental La:Mn ratio and high concentration of surface oxygen species.

5. Conclusions

$LaMnO_3$ and $La_{0.8}Sr_{0.2}MnO_3$ perovskites were synthesized by four different prep-

aration routes. It appeared that synthesis method affects physicochemical properties of obtained materials including catalytic activity in lean methane combustion. There is no simple answer to the question on the physicochemical reason for differences of catalytic behavior of studied perovskites. The use of solvothermal method allows one to obtain materials characterized by relatively well-developed surface area, the presence of reactive oxygen species on surface as well as high catalytic activity for lean methane combustion. Properties of the materials prepared by chemical combustion are very similar to that of solvothermally prepared. Spray pyrolysis leads to materials possessing the lowest specific surface area and porosity, characterized by the acidic character of the surface. LM and LSM perovskites prepared by the spray pyrolysis method show low susceptibility to reduction with H_2 and the highest share of lattice oxygen on the surface which can be correlated with the lowest activity in lean methane combustion. LM and LSM prepared by sol-gel method exhibit an intermediate properties between that ones prepared by solvothermal (or chemical combustion) and spray pyrolysis. LSM perovskites prepared by solvothermal and spray pyrolysis have a less than stoichiometric content of Sr.

All prepared LM and LSM materials show catalytic activity for lean CH_4, comparable to (or higher) than the activity of 0.5 wt.% Pt/Al_2O_3 but lower than 1 wt.% Pd/Al_2O_3. Qualitatively catalytic activity of lean methane combustion on studied perovskites can be correlated with the presence of α and β oxygen forms on their surface as well as availability of these species and the degree of surface development. The rate of methane combustion on LM perovskites quite well correlates with temperature of first maximum of hydrogen consumption. In case of LSM perovskites neither results of TPR-O_2 nor TPR-H_2 could be simply correlated with rates of methane combustion. Catalytic properties of LSM prepared by MS are affected by lower than assumed content of strontium leading to high content of β-oxygen on its surface. These species desorb from the LSM-MS surface at relatively higher temperatures than in the case of other LSM materials what may results in lower rate of methane combustion at low temperatures range.

Acknowledgements

The work was financed by a statutory activity subsidy from the Polish Ministry of Science and Higher Education for the Faculty of Chemistry of Wrocław University of Technology. We would like to thank dr W. Miśta for the TPD O_2 measurements.

References

[1] U.S. Environmental Protection Agency (2008) Inventory of U.S. Greenhouse Gas Emission and Sinks 1990-2006. Washington DC.

[2] Su, S., Beath, A., Guo, H. and Mallett, C. (2005) An Assessment of Mine Methane Mitigation and Utilisation Technologies. *Progress in Energy and Combustion Science*, **31**, 123-170. https://doi.org/10.1016/j.pecs.2004.11.001

[3] Janbey, A., Clark, W., Noordally, E., Grimes, S. and Tahir, S. (2003) Noble Metal Catalysts for Methane Removal. *Chemosphere*, **52**, 1041-1046. https://doi.org/10.1016/S0045-6535(03)00292-3

[4] Okal, J. and Zawadzki, M. (2013) Catalytic Combustion of Methane over Ruthenium Supported on Zinc Aluminate Spinel. *Applied Catalysis A*: *General*, **453**, 349-357. https://doi.org/10.1016/j.apcata.2012.12.040

[5] Wei, H.J., Cao, Y., Au, W.J.J. and Au, C.T. (2008) Lattice Oxygen of $La_{1-x}Sr_xMO_3$ (M = Mn, Ni) and $LaMnO_{3-\alpha}F_\beta$ Perovskite Oxides for the Partial Oxidation of Methane to Synthesis Gas. *Catalysis Communications*, **9**, 2509-2514. https://doi.org/10.1016/j.catcom.2008.06.019

[6] Marchetti, L. and Forni, L. (1998) Catalytic Combustion of Methane over Perovskites. *Applied Catalysis B*: *Environmental*, **15**, 179-187. https://doi.org/10.1016/S0926-3373(97)00045-3

[7] Seyama, T. (1992) Total Oxidation of Hydrocarbons on Perovskite Oxides. *Catalysis Reviews*. *Science and Engineering*, **34**, 282.

[8] Borovskikh, L., Mazo, G. and Kemnitz, E. (2003) Reactivity of Oxygen of Complex Cobaltates $La_{1-x}SrxCoO_{3-\delta}$and $LaSrCoO_4$. *Solid State Sciences*, **5**, 409-417. https://doi.org/10.1016/S1293-2558(03)00052-9

[9] Fu, Q. and Wagner, T. (2007) Interaction of Nanostructured Metal Overlayers with Oxide Surfaces. *Surface Science Reports*, **62**, 431-498. https://doi.org/10.1016/j.surfrep.2007.07.001

[10] Martin, D. and Duprez, D. (1996) Mobility of Surface Species on Oxides. 1. Isotopic Exchange of $^{18}O_2$ with ^{16}O of SiO_2, Al_2O_3, ZrO_2, MgO, CeO_2, and CeO_2-Al_2O_3. Activation by Noble Metals. Correlation with Oxide Basicity. *The Journal of Physical Chemistry*, **100**, 9429-9438. https://doi.org/10.1021/jp9531568

[11] Royer, S., Bérubé, F. and Kaliaguine, S. (2005) Effect of the Synthesis Conditions on the Redox and Catalytic Properties in Oxidation Reactions of $LaCo_{1-x}Fe_xO_3$. *Applied Catalysis A*: *General*, **282**, 273-284. https://doi.org/10.1016/j.apcata.2004.12.018

[12] Gao, Z. and Wang, R. (2010) Catalytic Activity for Methane Combustion of the Perovskite-Type $La_{1-x}Sr_xCoO_{3-\delta}$ Oxide Prepared by the Urea Decomposition Method. *Applied Catalysis B*: *Environmental*, **98**, 147-153. https://doi.org/10.1016/j.apcatb.2010.05.023

[13] Chiarello, G.L., Rossetti, I. and Forni, L. (2005) Flame-Spray Pyrolysis Preparation of Perovskites for Methane Catalytic Combustion. *Journal of Catalysis*, **236**, 251-261. https://doi.org/10.1016/j.jcat.2005.10.003

[14] Teng, F., Han, W., Liang, S., Gaugeu, B., Zong, R. and Zhui, Y. (2007) Catalytic Behavior of Hydrothermally Synthesized $La_{0.5}Sr_{0.5}MnO_3$ Single-Crystal Cubes in the Oxidation of CO and CH_4. *Journal of Catalysis*, **250**, 1-11. https://doi.org/10.1016/j.jcat.2007.05.007

[15] Najjar, H., Lamonier, J.-F., Mentre, O., Giraudon, J.M. and Batis, H. (2011) Optimization of the Combustion Synthesis towards efficient $LaMnO_{3+y}$ Catalysts in Methane Oxidation. *Applied Catalysis B*: *Environmental*, **106**, 149-159.

[16] Zhang, C.H., Guo, Y., Lu, G., Boreave, A., Retailleau, L., Baylet, A. and Giroir-Fendler, A. (2014) $LaMnO_3$ Perovskite Oxides Prepared by Different Methods for Catalytic Oxidation of Toluene. *Applied Catalysis B*: *Environmental*, **148**-**149**, 490-498. https://doi.org/10.1016/j.apcatb.2013.11.030

[17] http://ziemianarozdrozu.pl/encyklopedia/38/energia-i-emisje-co2

[18] http://ekoproblemy.cba.pl/efciepl.htm

[19] http://www.plazma.efuturo.pl/poster1.htm

[20] Grzybowska-Świerkosz, B. (1993) Elementy Katalizy Heterogenicznej. Wydawnictwo Naukowe PWN, Warszawa.

[21] Merino, N.A., Barbero, B.P., Eloy, P. and Cadús, L.E. (2006) $La_{1-x}Ca_xCoO_3$ Perovskite-Type Oxides: Identification of the Surface Oxygen Species by XPS. *Applied Surface Science*, **253**, 1489-1493. https://doi.org/10.1016/j.apsusc.2006.02.035

[22] Martin, D. and Duprez, D. (1997) Evaluation of the Acid-Base Surface Properties of Several Oxides and Supported Metal Catalysts by Means of Model Reactions. *Journal of Molecular Catalysis A*: *Chemical*, **118**, 113-128. https://doi.org/10.1016/S1381-1169(96)00371-8

[23] Kaddouri, A. and Ifrah, S. (2006) Microwave-Assisted Synthesis of $La_{1-x}B_xMnO_{3.15}$ (B = Sr, Ag; x = 0 or 0.2) via Manganese Oxides Susceptors and Their Activity in Methane Combustion. *Catalysis Communications*, **7**, 109-113. https://doi.org/10.1016/j.catcom.2005.09.010

[24] Buciuman, F.C., Patcas, F., Menezo, J.-C., Barbier, J., Hahn, T. and Lintz, H.-G. (2002) Catalytic Properties of $La_{0.8}A_{0.2}MnO_3$ (A = Sr, Ba, K, Cs) and $LaMn_{0.8}B_{0.2}O_3$ (B = Ni, Zn, Cu) Perovskites: 1. Oxidation of Hydrogen and Propene. *Applied Catalysis B*: *Environmental*, **35**, 175-183. https://doi.org/10.1016/S0926-3373(01)00250-8

[25] Alifanti, M., Kirchnerova, J. and Delmon, B. (2003) Effect of Substitution by Cerium on the Activity of $LaMnO_3$ Perovskite in Methane Combustion. *Applied Catalysis A: General*, **245**, 231. https://doi.org/10.1016/S0926-860X(02)00644-0

[26] Rosso, I., Garrone, E., Geobaldo, F., Onida, B., Saracco, G. and Specchia, V. (2001) Sulphur Poisoning of $LaMn_{1-x}Mg_xO_3$ Catalysts for Natural Gas Combustion. *Applied Catalysis B*: *Environmental*, **30**, 61-73. https://doi.org/10.1016/S0926-3373(00)00222-8

[27] Ponce, S., Peña, M.A. and Fierro, J.L.G. (2000) Surface Properties and Catalytic Performance in Methane Combustion of Sr-Substituted Lanthanum Manganites. *Applied Catalysis B*: *Environmental*, **24**, 193-205. https://doi.org/10.1016/S0926-3373(99)00111-3

[28] Hernández, W.Y., Tsampas, M.N., Zhao, C., Boreave, A., Bosselet, F. and Vernoux, P. (2015) La/Sr-Based Perovskites as Soot Oxidation Catalysts for Gasoline Particulate Filters. *Catalysis Today*, **258**, 525-534. https://doi.org/10.1016/j.cattod.2014.12.021

[29] Kaliaguine, S., van Neste, A., Szabo, V., Gallot, J.E., Bassir, M. and Muzychuk, R. (2001) Perovskite-Type Oxides Synthesized by Reactive Grinding: Part I. Preparation and Characterization. *Applied Catalysis A*: *General*, **209**, 345-358. https://doi.org/10.1016/S0926-860X(00)00779-1

[30] Melo, D.M.A., Borges, F.M.M., Ambrosio, R.C., Pimentel, P.M., da Silva Júnior, C.N. and Melo, M.A.F. (2006) XAFS Characterization of $La_{1-x}Sr_xMnO_{3\pm\delta}$ Catalysts Prepared by Pechini's Method. *Chemical Physics*, **322**, 477-484. https://doi.org/10.1016/j.chemphys.2005.09.008

[31] Pilania, G. and Ramprasad, R. (2010) Adsorption of Atomic Oxygen on Cubic $PbTiO_3$ and $LaMnO_3$ (001) Surfaces: A Density Functional Theory Study. *Surface Science*, **604**, 1889-1893. https://doi.org/10.1016/j.susc.2010.07.021

[32] Zhou, Y., Lü, Z., Wei, B., Wang, Z. and Zhu, X. (2015) Electronic Structure and Surface Properties of $PrMnO_3$ (001): A Density Functional Theory Study. *Solid State Communications*, **201**, 31-35. https://doi.org/10.1016/j.ssc.2014.10.005

[33] http://www.poch.com.pl/1/wysw/utworz_pdf.php?nr_karty=1264

[34] Cimino, S., Lisi, L., De Rossi, S., Faticanti, M. and Porta, P. (2003) Methane Combustion and CO Oxidation on $LaAl_{1-x}Mn_xO_3$ Perovskite-Type Oxide Solid Solutions. *Applied Catalysis B*: *Environmental*, **43**, 397-406. https://doi.org/10.1016/S0926-3373(03)00023-7

[35] Nagabhushana, B.M., Sreekanth Chakradhar, R.P., Ramesh, K.P., Shivakumara, C. and Chandrappa, G.T. (2006) Low Temperature Synthesis, Structural Characterization, and Zero-Field Resistivity of Nanocrystalline $La_{1-x}Sr_xMnO_{3+\delta}$ ($0.0 \le x \le 0.3$) Manganites. *Materials Research Bulletin*, **41**, 1735-1746. https://doi.org/10.1016/j.materresbull.2006.02.014

[36] Royer, S., Alamdari, H., Duprez, D. and Kaliaguine, S. (2005) Oxygen Storage Capacity of La_{1-x} A'_xBO_3 Perovskites (with A' = Sr, Ce; B = Co, Mn)—Relation with Catalytic Activity in the CH_4 Oxidation Reaction. *Applied Catalysis B*: *Environmental*, **58**, 273-288. https://doi.org/10.1016/j.apcatb.2004.12.010

[37] Yamazoe, N. and Teraoka, Y. (1990) Oxidation Catalysis of Perovskites—Relationships to Bulk Structure and Composition (Valency, Defect, etc.). *Catalysis Today*, **8**, 175-199. https://doi.org/10.1016/0920-5861(90)87017-W

[38] van Roosmalen, J.A.M., Cardfunke, E.H.P., Helmholdt, R.B. and Zandbergen, H.W. (1994) The Defect Chemistry of $LaMnO_{3\pm\delta}$: 2. Structural Aspects of $LaMnO_{3+\delta}$. *Journal of Solid State Chemistry*, **110**, 100-105. https://doi.org/10.1006/jssc.1994.1141

[39] Royer, S., Berube, F. and Kaliaguine, S. (2005) Effect of the Synthesis Conditions on the Redox and Catalytic Properties in Oxidation Reactions of $LaCo_{1-x}Fe_xO_3$. *Applied Catalysis A*: *General*, **282**, 273-284. https://doi.org/10.1016/j.apcata.2004.12.018

[40] Worayingyong, A., Kangvansura, P., Ausadasuk, S. and Praserthdam, P. (2008) The Effect of Preparation: Pechini and Schiff Base Methods, on Adsorbed Oxygen of $LaCoO_3$ Perovskite Oxidation Catalysts. *Colloids and Surfaces A*: *Physicochemical and Engineering Aspects*, **315**, 217-225. https://doi.org/10.1016/j.colsurfa.2007.08.002

[41] Cherkezova-Zheleva, Z., Paneva, D., Yordanova, I., Shopska, M. and Kolev, H. (2014) Mechanochemical Preparation and Properties of Nanodimensional Perovskite Materials. *Acta Physica Polonica A*, **126**, 916-920. https://doi.org/10.12693/APhysPolA.126.916

[42] Najjar, H. and Batis, H. (2010) La-Mn Perovskite-Type Oxide Prepared by Combustion Method: Catalytic Activity in Ethanol Oxidation. *Applied Catalysis A*: *General*, **383**, 192-201. https://doi.org/10.1016/j.apcata.2010.05.048